EFFECTS OF PERIODIC UNSTEADINESS OF A ROCKET ENGINE PLUME ON THE PLUME-INDUCED SEPARATION SHOCK WAVE*

Julian O. Doughty
The University of Alabama, Tuscaloosa

SUMMARY

A wind-tunnel investigation was conducted to study the flow field in which separation is caused by an expanding plume, with emphasis on effects associated with periodic unsteadiness in the plume. The separation shock was photographed with high-speed motion pictures, from which mean shock position and excursion data are reported. Pressure fluctuations were measured beneath the separation shock and statistics of the results are reported. A response of the separation shock to plume periodic unsteadiness was identified, and the magnitude of a corresponding transfer function was defined and is reported.

INTRODUCTION

A rocket booster vehicle will typically have a significantly under-expanded engine exhaust in the latter duration of its burn. The exhaust then plumes to a large diameter and alters the vehicle flow field considerably. Significantly, the plume is usually large at the altitude where the vehicle encounters maximum dynamic pressure.

When a large plume is generated by a vehicle in supersonic flight, it causes separation of the vehicle boundary layer well forward of the plume itself, and a separation shock wave radiates from a position near the separation point. The flow field is illustrated in figure 1. An inherent unsteadiness exists for this flow field as is often experienced in rigid surface compression corner flow at large Reynolds numbers. (For example, see references 1,2,3, and 4.) Separation shock excursions of several meters were reported by Jones from in-flight observations of a Saturn V vehicle (ref. 5). One would expect rather severe surface pressure fluctuations to accompany such shock motion.

Since large liquid fuel rocket engines exhibit a periodic unsteadiness, the question of that influence on the separation shock excursions and the resulting surface pressures becomes one of importance. This paper

*The research presented in this paper was supported by the National Aeronautics and Space Administration under Contract No. NAS8-30624.

presents some results of a wind-tunnel simulation of plume-induced flow separation with and without periodic plume unsteadiness.

SYMBOLS

Values are given in SI Units. The measurements and calculations were made in U.S. Customary Units.

F	plume forcing, atm^2
f	frequency, Hz
G	power spectral density, atm^2-sec
$\|H(f)\|$	transfer function magnitude
q	test-section dynamic pressure, atm
R	response to periodic plume unsteadiness, atm^2
U	test-section freestream velocity, m/sec
x	shock position, cm (figure 1)
$\bar{x}$	mean shock position, cm
δ	boundary-layer thickness, cm
θ	shock angle, deg (figure 1)
σ	standard deviation, cm

MODEL AND TEST FACILITIES

Model Description

The basic configuration of the model used in this study is a cone-cylinder body which uses secondary air flow to produce a plume near the aft end. (See figure 2.) The model is wall-mounted with its axis of symmetry located at the wind-tunnel wall boundary-layer displacement thickness as calculated by the method of Maxwell and Jacocks (ref. 6). This mounting arrangement was selected to provide access for the secondary plume flow and to minimize the distance from the generation of the plume unsteadiness (plume pulsing) and the plume itself. (The significance of minimizing this distance will be discussed later.)

Stainless steel fins are used to isolate the plume to a sector. The

upper fin surfaces extend into the plume nozzle and settling chamber so that all model geometry in the sector between the fins is that of a body of revolution. Therefore, flow in the sector between the fins simulates true axisymmetric flow except for the boundary layer on the fin surfaces, and the distance from the fin leading edge to the separation shock is kept small to minimize the boundary-layer effect. The leading edge of the fin is sharp, beveled away from the flow sector. A dihedral angle, limited by line-of-sight requirements across the top of the model, is set into the fins to remove them from the tunnel wall boundary layer. Oil flow studies, pressure measurements on the upper model surface, and Schlieren studies were conducted to assure that axisymmetric flow had been realized. All indications were positive except for some flow angularity in a small region at the fin-cylinder intersection. A lightly knurled band is located just behind the cone-cylinder intersection to promote a turbulent boundary layer.

Plume Generation

The plume is generated by secondary flow directed through the tunnel wall into a settling chamber in the core of the plume (figure 3). Flow from the settling chamber issues through the nozzle which is formed by two conical surfaces sharing a common vertex. Therefore, the nozzle flow is approximately spherical source flow, and it has an isentropic exit Mach number of 2.94. The solid core in the plume center not only provides space for a settling chamber and instrumentation, but also greatly reduces the secondary mass flow required while still generating the required forward plume surface for the study. Without the plume core the secondary mass flow requirements would have presented severe problems in terms of the physical size of the supply ports.

Plume Pulsing

Pulsing or periodic unsteadiness was induced in the plume stagnation pressure by a periodic partial relief of the plume supply air. This was accomplished by periodically diverting a part of the plume supply air to the atmosphere. The apparatus for doing this was a variable-speed rotating disk with evenly spaced holes on a circumference which aligned with a teflon orifice which was teed off the plume air supply. Pulse frequency was controlled by the disk rotational speed and the pulse magnitude was controlled by the orifice size. The arrangement is shown in figure 3.

The pressure signal, measured in the plume settling chamber, generated by the pulsing apparatus was that of a periodic component superimposed on a larger steady component. The periodic part was approximately a sine wave, especially for cases in which the orifice size was about the same as the disk holes. The wave was somewhat like a "flattened sine wave" for tests in which the orifice was considerable smaller than the disk holes.

The time required for a pulse to travel from the orifice to the plume settling chamber places an upper limit on the frequency for which a good pressure signal can be generated. In this experiment the distance from the orifice to the settling chamber was approximately 10 cm, and wave distortion

was evident at frequencies above 500 or 600 Hz. At 1000 Hz the distortion was severe. A periodic wave was produced but with a greatly reduced amplitude and an appearance more like a rectified sine wave. It was assumed that individual pulses were interfering with each other. Data reported here are for frequencies well below the distortion range.

Instrumentation

Surface pressure fluctuations at the separation shock were measured by a flush-mounted strain-gage-type transducer with a diameter of 2 mm and a natural frequency above 100 kHz. The static pressure level was eliminated by feeding the signal from a surface orifice, located laterally adjacent to the transducer, through a 3 m length of tubing to the reverse side of the transducer diaphragm. The length of tubing filtered the fluctuations and provided a time-average reference so that the transducer sensed only the fluctuations. This technique was suggested by Mr. L. Muhlstein, Jr. of Ames Research Center, who was also kind enough to supply filtering data.

Plume pressure fluctuations were measured by a crystal-type transducer located in the plume settling chamber. All fluctuating pressure data were stored on magnetic tape for subsequent reduction.

Separation shock geometric data were taken from high-speed Schlieren motion pictures taken at 800 frames per second with an exposure of 0.002 seconds. Measurements were then made by single frame projection of the resulting film onto a grid.

Boundary-layer thickness was measured by using two parallel stagnation probes mounted on a micrometer locater. The edge of the boundary layer was identified as the position, nearest the body, for which the pressures balanced.

Wind Tunnel

The wind tunnel used in this project was a blowdown supersonic tunnel with a 16-by 16-cm test section, located at The University of Alabama, Tuscaloosa. A major part of the data collection and reduction was done by Messers J. D. Dagen and F. L. Smith.

Test Conditions

All data reported are for the following freestream conditions:

Mach no. = 2.9

airspeed = 607 m/sec

stagnation temperature = 288 to 294 K

static pressure = 0.151 atm

stagnation pressure = 4.76 atm

dynamic pressure = 0.878 atm

Reynolds no. = 4.9×10^7 per meter.

The plume stagnation pressure was nominally 33 atm. That value located the mean position of the separation shock on the surface pressure transducer and generated a characteristic signal which could readily be identified on an oscilloscope.

RESULTS

Separation Shock Excursion

Observation and measurements from the high-speed motion pictures showed that the separation shock was in constant motion, regardless of whether or not there was plume pulsing. As it moved, it maintained essentially a constant shock angle with the freestream. In these tests, the shock angle was 28 degrees and mean shock location, $\bar{x}$, was 5.87 cm. In this context, shock location and separation length are taken to be the same (see figure 1). Histograms of shock excursion for a steady plume and for four different pulsing frequencies are shown in figure 4. Each histogram represents 4,000 measured positions. The root-mean-square level of plume pressure pulses for these data is 4.3 percent of the plume stagnation pressure.

There are no distinctions among the histograms which could not be attributed to experimental error and the finite data sample. The magnitude of plume pulsing used was sufficient to produce obvious distinctions in the surface pressure power spectra associated with the separation shock excursions (to be discussed later). Therefore, if any effect exists of plume unsteadiness on the shock excursion histogram, it is rather subtle.

The motion pictures of shock travel were viewed at several different frame speeds. It was not possible to distinguish the effect of plume pulsing in this manner. In all instances the impression from viewing movement of the shock was that it jumps from one position of momentary stability to another in an apparently random manner.

Fluctuating Pressure Power Spectra

One of the most obvious effects of periodic plume unsteadiness appears on the power spectrum of the surface pressure beneath the separation shock. A spike, located at the pulsing frequency, is generated in the spectrum, (see figures 5 and 6). Figure 5 shows the pressure signals as taken directly from a one-third octave filtering system, and figure 6 shows power spectra of the

same data normalized as suggested by Coe* (ref. 1). The spike is produced by 80 Hz plume pulsing at an RMS level of 3.76 percent of the plume stagnation pressure. The broadband level of the basic spectrum (unpulsed) is 166.6 dB and that of the spectrum associated with 80 Hz pulsing is 166.9 dB.

Comparing the spectra and noting that the broadband (integrated) levels are the same leads to the conclusion that the spike is formed at the expense of the balance of the spectrum. In fact, within the limits of data scatter, this conservation of the spectrum integral, with respect to periodic plume pulsing at various frequencies and strengths, has been observed in all instances (over 100 tests) in the course of this project.

Response to Plume Pulsing

For the purpose of quantitatively relating plume unsteadiness to the pressure fluctuations at the foot of the separation shock, the plume forcing magnitude is defined to be that area under the resulting spectrum spike which is above the spectrum with the spike faired out. In determining the area under the spike, each one-third-octave band produces a rectangular area consistent with the filter process by which the spectrum is produced. This is not withstanding the fact that it is often the practice to connect the points with a curve to display the spectrum. The quantities identified as "forcing" and "response" are clearly not the only ones which could have been chosen. Since there is some arbitrariness, the "best" definitions will likely vary according to personal preference and situation. However, it is hoped that the definitions selected are reasonable and useful.

With the definitions stated, the response to periodic plume unsteadiness is displayed in figure 7. Within experimental error, over the range tested, a linear relationship exists which is independent of pulse frequency. The results can be expressed in terms of a transfer function if it is postulated that forcing and response are reasonably represented by a linear differential equation. Then the magnitude of the transfer function is

$$|H(f)| = \sqrt{\frac{R(f)}{F(f)}} = 0.0169 \qquad (16\text{Hz} \leq f \leq 250\ \text{Hz}), \tag{1}$$

and is constant for these data.

---

*Except that Coe used δ measured just ahead of the shock, whereas in this case δ was measured at the shock location, but in the absence of a plume and consequently a separation shock. For these data, δ = 0.53 cm.

CONCLUDING REMARKS

Several effects associated with plume-induced flow separation have been identified. The following statements are applicable over the range of this study:

1. The separation shock exhibits an excursion about some mean location and maintains essentially constant direction as it moves. This is true with or without plume unsteadiness.

2. The probability that the separation shock is located in a given position interval at a given instant is not influenced by plume unsteadiness.

3. Periodic plume unsteadiness produces a spike on the separation shock surface pressure power spectrum. The spike strength is proportional to the plume pulsing magnitude. The proportionality is constant over a frequency range.

4. The broadband level of the separation shock surface pressure fluctuations is not affected by periodic plume unsteadiness, so that the spectrum spike is produced at the expense of the balance of the spectrum.

REFERENCES

1. Coe, C. F.: Surface-Pressure Fluctuations Associated with Aerodynamic Noise. NASA SP-207, 1969, pp. 409-424.

2. Coe, C. F. and Chye, W. J.: Pressure-Fluctuation Inputs and Response of panels Underlying Attached and Separated Supersonic Turbulent Boundary Layers. NASA TM X-62, 189, 1972.

3. Kistler, A. L.: Fluctuating Wall Pressure Under a Separated Supersonic Flow. J. Acoust. Soc. Am., Vol. 36, No. 3, 1964, p. 543.

4. Trilling, L.: Oscillating Shock Boundary-Layer Interactions. J. Aero. Sci., May 1958, pp. 301-304.

5. Jones, J. H.: Acoustic Environmental Characteristics of the Space Shuttle. Proc. Space Shuttle Technology Conf., July 1970.

6. Maxwell, H. and Jacocks, J. L.: Nondimensional Calculation of Turbulent Boundary-Layer Development in Two-Dimensional Nozzles of Supersonic Wind Tunnels. AEDC-TN-61-153, 1962.

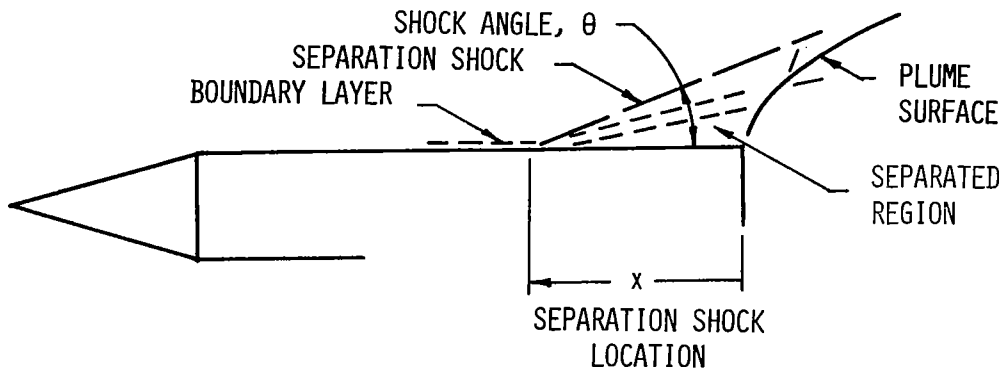

Figure 1.- Plume-induced flow separation.

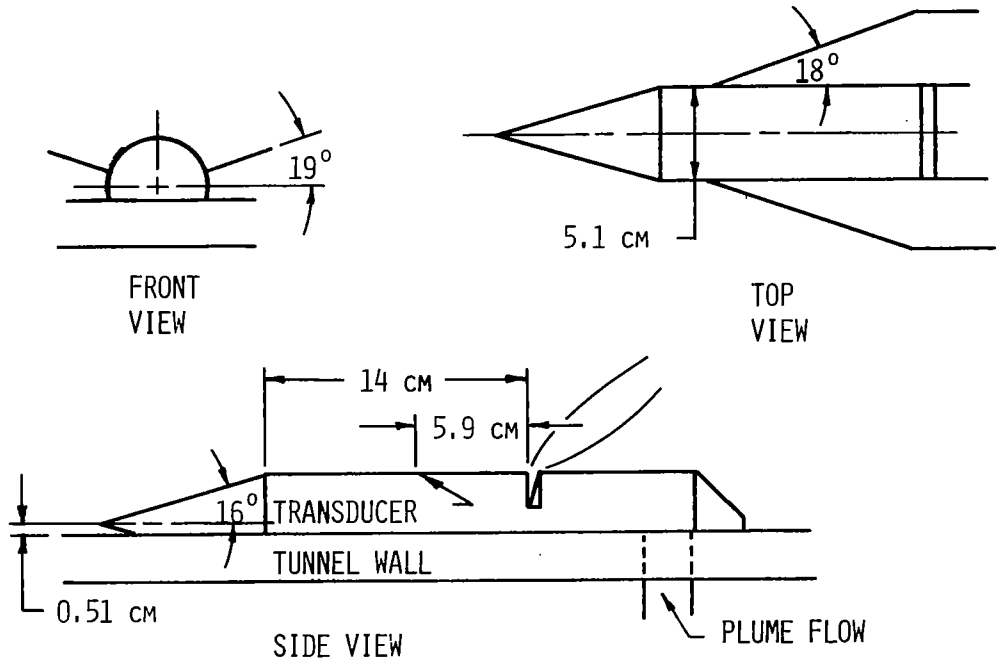

Figure 2.- The test model.

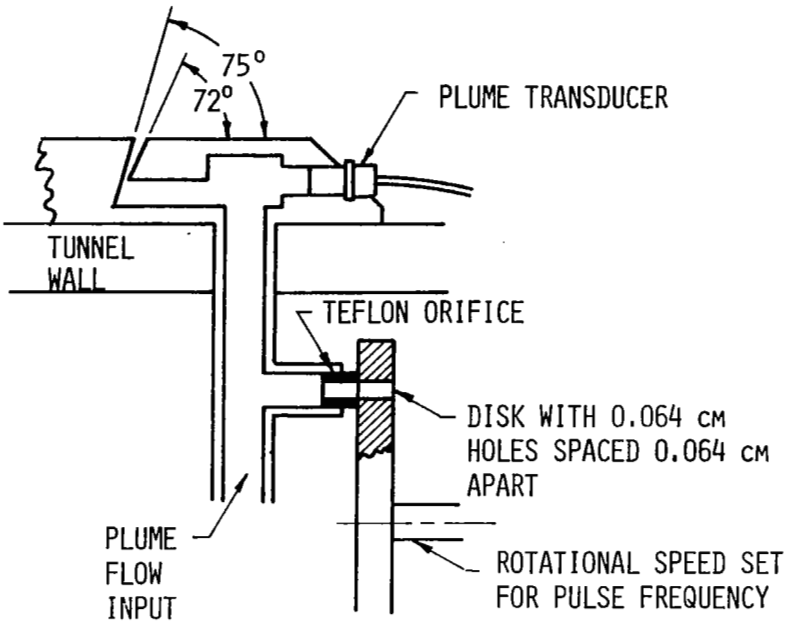

Figure 3.- Plume generation details.

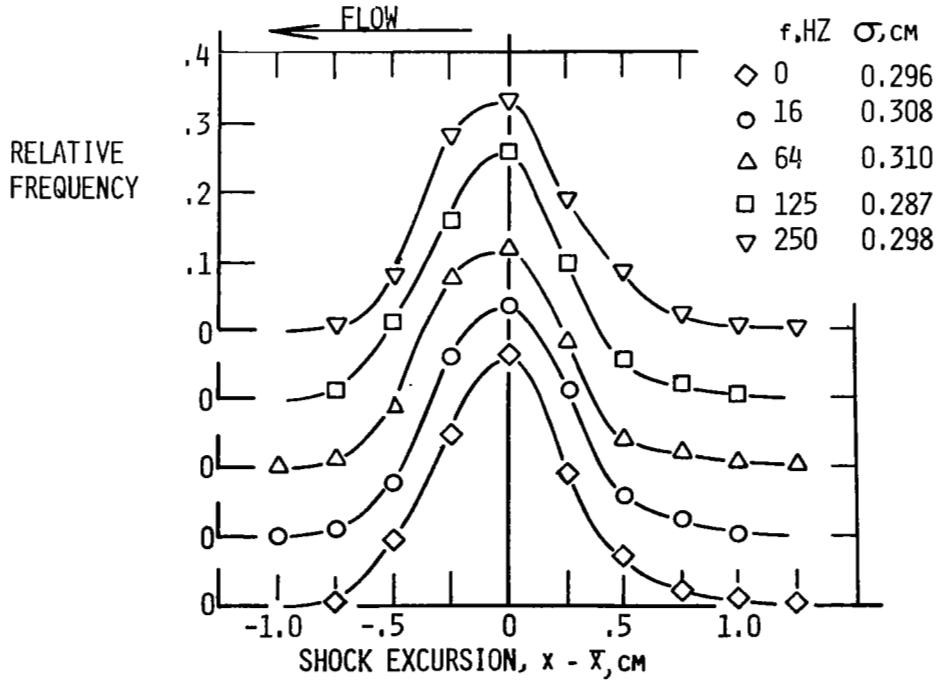

Figure 4.- Effect of plume pulse frequency on shock excursions.

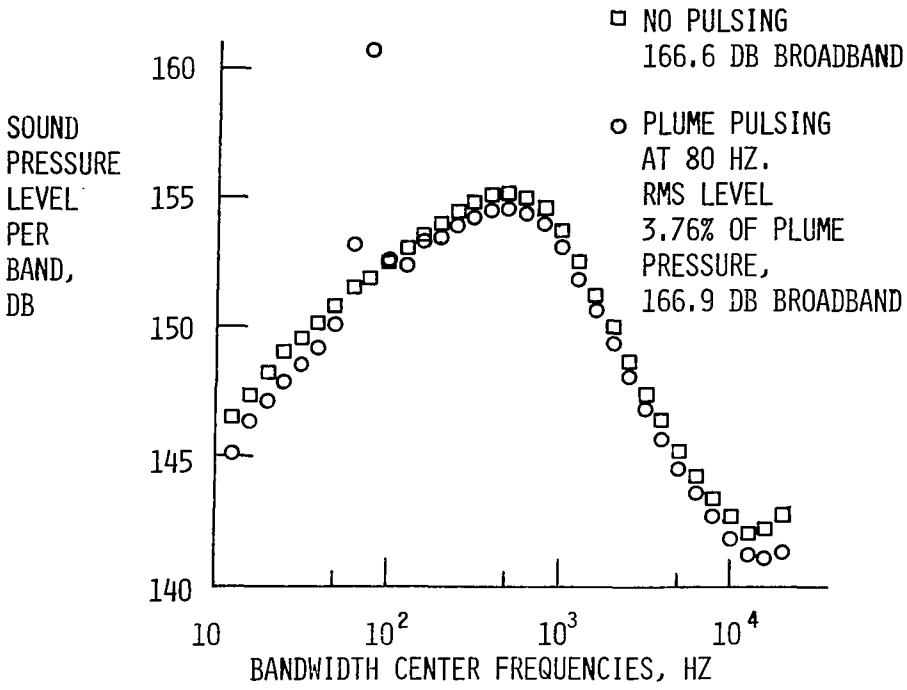

Figure 5.- Shock fluctuation pressure raw data.

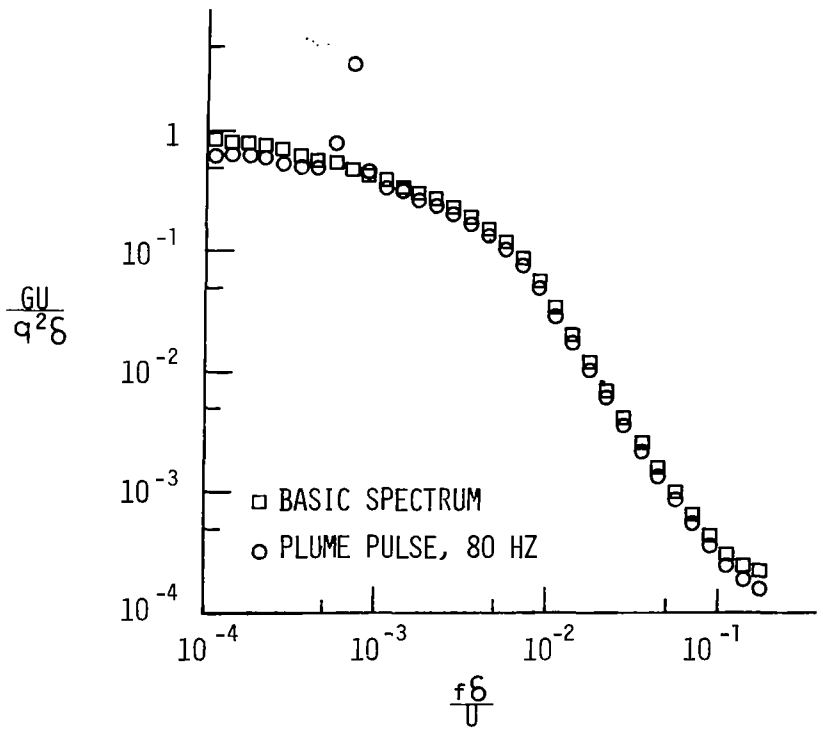

Figure 6.- Shock power spectra.

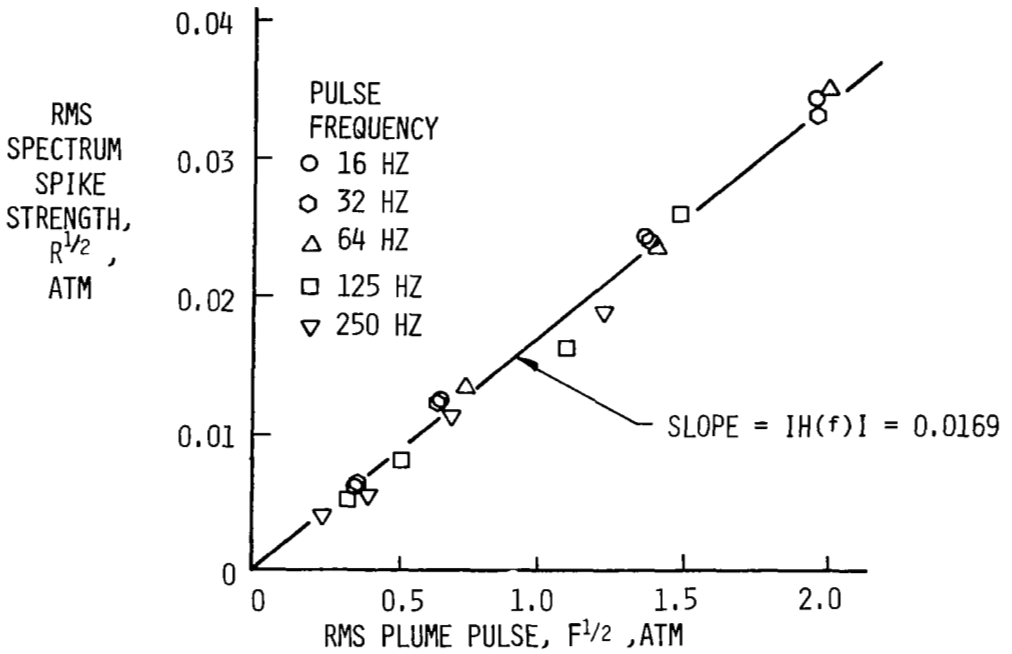

Figure 7.- Power spectra response to plume pulsing.